Degradation of Methylene Blue Dye Using ZnO/$NiFe_2O_4$ Photocatalyst Under Visible Light

Yuniar Yuniar[1], Tri Mawarni[2], Poedji Loekitowati Hariani[3], Muhammad Faizal[1], Tuty Emilia Agustina[1,*]

[1] *Department of Chemical Engineering, Faculty of Engineering, Sriwijaya University, Palembang, Indonesia*
[2] *Department of Chemical Engineering Department, State Polythecnic Sriwijaya, Palembang, Indonesia*
[3] *Department of Chemistry, Faculty of Mathematic and Natural Science, Sriwijaya University, Palembang, Indonesia*
[*] *Corresponding author. Email: tuty_agustina@unsri.ac.id*

ABSTRACT
The effective synthesis of ZnO/$NiFe_2O_4$ photocatalyst with a co-precipitation technique was used to degrade dyes in the air in this study. XRD, SEM-EDS, and other equipment are used to characterize the crystalline phase, surface morphology, and chemical composition of photocatalysts. The exact peaks of the nanocomposite XRD pattern corresponded to cubic spinel $NiFe_2O_4$ and hexagonal wurtzite ZnO, according to the results. At a $NiFe_2O_4$ to ZnO molar ratio of 2:0.1, all nanocomposites demonstrated photocatalytic activity in decomposing methylene blue dye 50 ppm higher than pure ZnO. After 40 minutes of exposure to visible light, the product demonstrated photocatalytic activity, with a degradation efficiency of 92 percent.

Keywords: *Degradation, photocatalyst, metilen blue, ZnO/$NiFe_2O_4$*

1. INTRODUCTION

The use of semiconductors in the photocatalysis process is an environmentally friendly, low-cost technology for removing organic pollutants by dissociating organic pollutants into CO_2, H_2O, or air and thereby helping to reduce environmental pollution [1]. ZnO [2], TiO_2 [3], CdS [4], and CeO_2 [5] are some of the semiconductors used in photocatalysis. Photocatalyst semiconductor with high photocatalytic efficiency and the ability to convert light energy into chemical energy at a low cost. Among the semiconductors mentioned above, ZnO nanoparticles are thought to be photocatalyst semiconductors that are easily adapted for photooxidation of organic pollutants [6].

Zinc oxide is an environmentally friendly material that has no negative effects on organism life, human health, or the environment. In comparison to other metal-oxide semiconductors, ZnO has a direct and wide-bandgap in the near UV spectrum region, as well as a high efficiency in removing and completely degrading pollutants and the ability to absorb a broad spectrum of visible light [7]. However, the ZnO photocatalyst process mostly uses UV light sources because the ZnO bandgap energy is quite large, namely 3.37 eV so that when using sunlight it is less efficient because it only uses ± 5% of the sunlight spectrum (UV fraction of sunlight) [8]. The current use of UV lamps poses a serious problem due to high energy consumption which increases the operating costs of ZnO photocatalytic systems. Several researchers have made modifications to increase photocatalytic activity including Fe_3O_4/ZnO/graphene oxide [9], ZnO/$ZnFe_2O_4$ [10], ZnO/$MnFe_2O_4$ [11], ZnO/$NiFe_2O_4$ [12]. Modification of the ZnO photocatalyst that can use visible light for its activation will eliminate the limitations of using ZnO to degrade organic pollutants in the application of methylene blue dye processing in textile wastewater, besides that ZnO made in the form of nanoparticles can have greater energy than ordinary size materials because it has a large surface area.

Nickel ferrite ($NiFe_2O_4$) is a significant ferrite spinel due to its high saturation magnetization and narrow bandgap (1.6 eV). The combination of ZnO and $NiFe_2O_4$ results in a photocatalyst semiconductor that increases activity when exposed to visible light. In theory, when ferrite materials are combined with ZnO, heterojunctions are formed, and the electrons and holes produced by photogeneration are efficiently separated, resulting in an increase in photocatalytic activity. According to Jamarun and Arief [12], the combination

of ferromagnetic $NiFe_2O_4$ and a diamagnetic ZnO semiconductor results in superparamagnetic properties in the synthesized material. This ZnO/ $NiFe_2O_4$ composite's superparamagnetic nature aids in the separation of the catalyst from the liquid. These nanocomposites can be used to degrade dyes under visible light (400-700 nm).

The main species that can degrade are OH radicals and h+ photo-producing holes [13]. Another advantage of the ZnO/NiFe2O4 photocatalyst is that it can be recycled. Using a combination of hydrothermal and coprecipitation methods, $NiFe_2O_4$/ZnO nanocomposites have demonstrated that an effective solution is a photocatalyst of $NiFe_2O_4$/ZnO nanocomposites with high magnetization [14]. The co-precipitation method was used to create ZnO/ $NiFe_2O_4$ nanocomposites in this study, with chloride salt as the starting material. Photocatalyst was used to test the sample's ability to degrade methylene blue dye under visible light. The weight of the catalyst and the contact time have an effect on photodegradation.

2. EXPERIMENT PROCEDURE

2.1. Materials

The materials used are $ZnCl_2$, NaOH, $FeCl_2$ $4H_2O$, $FeCl_3.6H_2O$, $NiCl_2.6H_2O$, deionized water, distillate water, PEG 4000 and methylene blue (MB).

2.2. Equipment

X-ray diffraction (XRD) is the technology used. Scanning Electron Microscope-Energy Dispersive X-Ray (SEM-EDX) morphology of nanocomposite. UV-visible spectroscopy was used to determine the concentrations of methylene blue and methyl orange. A magnetic stirrer, furnace, centrifuge, LED lamp, and glassware are all part of the laboratory analysis equipment.

2.3. Methods

2.3.1. Synthesis of ZnO

Nanoparticles (NPs) ZnO was synthesized using the direct precipitation method [10]. Separate solutions of $ZnCl_2$ 1M and NaOH 2M were prepared by dissolving them in deionized water. The NaOH solution was added dropwise into the $ZnCl_2$ solution and stirred constantly for 2 hours at room temperature with a magnetic stirrer at 400 rpm to form a white suspension. After 2 hours of stirring, the white precipitate was centrifuged at 5000 rpm for 20 minutes to separate it from the solution. The product was then washed three times with deionized water to neutralize the pH, followed by absolute alcohol. Following that, the white precipitate was calcined in a furnace at 500ºC for 2 hours to form ZnO.

Reaction :

$$ZnCl_2 + 2NaOH \longrightarrow Zn(OH)_2 + 2NaCl$$

$$Zn(OH)_2 \longrightarrow ZnO + H_2O$$

2.3.2. Synthesis of $NiFe_2O_4$ Nanoparticle

Nickel ferrite ($NiFe_2O_4$) nanoparticle were synthesized using the chemical co-precipitation method reported by [13]. The chemical reaction is illustrated as follows :

$$NiCl_2 + 2FeCl_3 + 8NaOH \longrightarrow NiFe_2O_4 + 8NaCl + 4H_2O$$

In brief, deionized water was used to prepare $NiCl_2.6H_2O$ 0.2 M and $FeCl_3.6H_2O$ 0.4 M solutions. The two solutions were mixed in the same volume and quickly stirred for 1 hour at 80°C with a magnetic stirrer. Drop by drop, 2M NaOH was added to the solution until it reached pH 12 and a brown precipitate formed. The precipitate was separated using a permanent magnet, washed with deionized water to neutrality, and dried in a 150°C oven for 2 hours. The dried $NiFe_2O_4$ nanoparticles were ground and sieved through a 200 mesh sieve.

2.3.3. ZnO/$NiFe_2O_4$ nanocomposites synthesis

ZnO/ $NiFe_2O_4$ was synthesized by varying the mole ratio of ZnO: $NiFe_2O_4$, namely 1: 0.1, 2: 0.1, and 3: 0.1, denoted by the symbols ZNi-1, ZNi-2, and ZNi-3. In 50 ml of distilled water, 2 g of ZnO and 1 g of PEG 4000 were dispersed and stirred at 500 rpm for 1 hour at 80 ºC. Then, 1.335 g of $FeCl_3.6H_2O$ and 0.587 g of $NiCl_2.6H_2O$ dissolved in 50 ml of distillate water were weighed and added to the ZnO-PEG mixture, stirred with drops of 2 M NaOH for 1 hour, and kept at 80ºC.

The resulting chocolate precipitate was centrifuged at 14000 rpm for 15 minutes. The precipitate was washed with deionized water until it reached a pH of neutral, then with absolute ethanol. The precipitate was calcined for 2 hours in a furnace at 500ºC to produce ZnO/$NiFe_2O_4$.

2.3.4. Characterization

ZnO, $NiFe_2O_4$, and ZnO/ $NiFe_2O_4$ nanocomposite were synthesized. X-ray diffraction (XRD; using XRD-D8 advanced ECO XRD system and SSD1601D detector, using Cu-K1 and K2 radiation) was used to examine the structure of the synthesized sample. The surface morphology and composition of samples were scanned using field emission scanning electron microscopy equipped with an energy dispersive X-ray (SEM-EDX EVO 18 Research), and the absorbance spectra of samples were recorded using a diffuse reflectance spectrophotometer UV-vis (Shimadzu UV-vis 2450 spectrophotometer).

2.3.5. Photocatalytic Activity

The photocatalytic activity of ZnO/ $NiFe_2O_4$ was tested by photodegrading the textile dye methylene blue. The experiment was conducted in a photoreactor with a Philips 10 W LED lamp. The catalytic experiment was carried out with constant stirring using 50 ml of methylene blue solution (50 ppm concentration) and 20 mg of ZnO/ $NiFe_2O_4$ nanocomposite catalyst powder. Approximately 5 ml of the aliquot solution was taken from the reaction mixture at 10, 20, 30, and 40 minute intervals, centrifuged, and the decrease in absorbance value was monitored using a UV-Vis spectrophotometer at 599 nm. The experiment was repeated with different amounts of catalyst, namely 5, 10, 15, 20, and 25 mg, while maintaining the dye solution concentration at 50 ppm. Under the same conditions, methylene blue was used without a catalyst in a control experiment. The degradation percentage of MB was calculated using the equation below.

Deradation (%) = ((Co – C)/Co) * 100%

3. RESULT AND DISCUSSION

3.1. Analysis of X-Ray Diffraction

XRD was used to examine the crystal structures of ZnO, $NiFe_2O_4$ nanoparticles, and ZNi-1, ZNi-2, and ZNi-3 nanocomposites synthesized via co-precipitation. The XRD pattern of ZnO, $NiFe_2O_4$, and ZNi-1, ZNi-2, and ZNi-3 nanocomposites is shown in Figure 1. The positions of sharp and narrow diffraction peaks with sample values of ZnO were observed at 2θ = 31.78, 34.42, 36.25, 47.54, 56.60, 62.86, 66.38, 67.96, 69.10, 72.56 and 76.96 indexed as hkl crystal planes namely (100), (002), (101), (102), (110), (103), (200), (112), (201), (004) and (202). This peak confirmed the formation of a wurtzite hexagonal crystal structure of ZnO nanoparticles. This peak corresponds to the hexagonal ZnO standard XRD data table of JCPDS No. 00-036-1451).

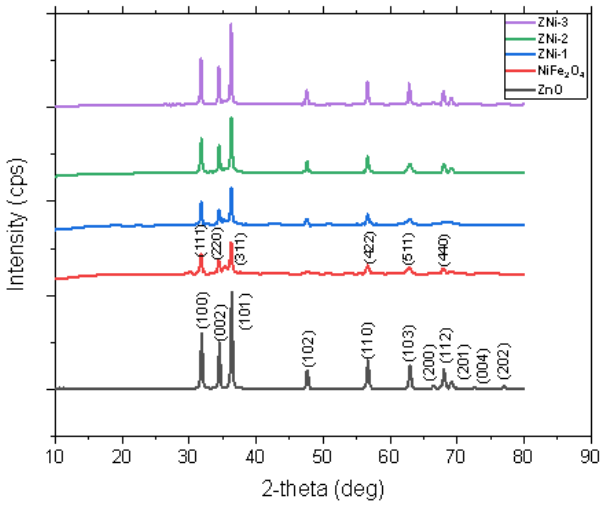

Figure 1. XRD Patterns

The diffraction peaks of $NiFe_2O_4$ nanorods show a highly oriented crystal structure of the spinel cubic. The positions of sharp and narrow diffraction peaks with sample values of $NiFe_2O_4$ appearing at 2θ are 21.39, 35.33, 41.70, 63.39, and 67.73 indexed as hkl crystal planes namely (111), (220), (311), (422), (440) and (511) corresponds to a cubic spinel. The obtained peak intensity profile is following pounder with JCPDS card No. 10-0325.

The XRD pattern of $NiFe_2O_4$ nanocomposites (ZNi-1, ZNi-2, and ZNi-3) matched the ZnO sample. Because of the small amount of NiFe2O4 and low crystallinity, the main diffraction peak of $NiFe_2O_4$ (2 = 36.25) is not observed for ZNi-1. As the amount of ZnO in the nanocomposite increases, the main peak of ZnO appears, as shown in ZNi-2 and ZNi-3. Using the Debey-Scherrer equation, the average crystal size of ZnO in nanocomposites (ZNi-1, ZNi-2, and ZNi-3) is estimated to be around 60 nm.

3.2. Elemental Morphology and Composition

The structural morphology of the photocatalyst was investigated using SEM-EDX analysis. Figure 2 shows SEM images of ZnO, NiFe2O4, and ZnO/ $NiFe_2O_4$. SEM images of $NiFe_2O_4$ nanorods reveal rod-shaped particles ranging in size from 30 to 40 nm. SEM image of hexagonal nanoparticles produced by co-precipitation synthesis of ZnO nanoparticles. These nanoparticles have a diameter of 40 nm. SEM analysis of ZNi-1, ZNi-2, and ZNi-3 revealed high agglomeration degrees and varying surface morphology.

The Magnetic Attraction Between Nickel Ferrite And Zinc Oxide Could Explain The Agglomeration And Different Morphology. Figure 2 Depicts The Edx Spectrum Of The Zni-2 Compositional Elements. Peaks Of The Elements Zn, O, Fe, And Ni Can Be Seen In This Spectrum With Percentages Of 68.10, 16.60, 10.92, And 4.38, Respectively. These Findings Indicate That $Nife_2o_4$ Has Been Combined With ZnO.

3.3. Photocatalytic Activity

The photocatalyst activity was evaluated by looking at the degradation results of methylene blue as an example of a dye in the the visible light. It was found that MB degradation increased rapidly with the addition of catalyst. From Figure 3a MB was degraded about 92% for 50 minutes in the presence of ZNi-1, ZNi-2, and ZNi-3 photocatalysts, respectively. Pure ZnO photocatalyst showed low activity in degrading MB.

The photocatalytic activity of the nanocomposite was found to be greater than that of ZnO and $NiFe_2O_4$. Under visible light irradiation, good photocatalytic activity using ZNi-2 nanocomposite photocatalyst can degrade 92% MB for 40 minutes. The mechanism for increasing the degradation of Percentage MB in the presence of the synthesized nanocomposite is as

follows: when exposed to visible light, electrons in the valence bands (CB) of $NiFe_2O_4$ and ZnO are excited to the conduction band (CB) separately, leaving a hole with a positive charge in the VB. Because of the band difference between $NiFe_2O_4$ and ZnO. ,

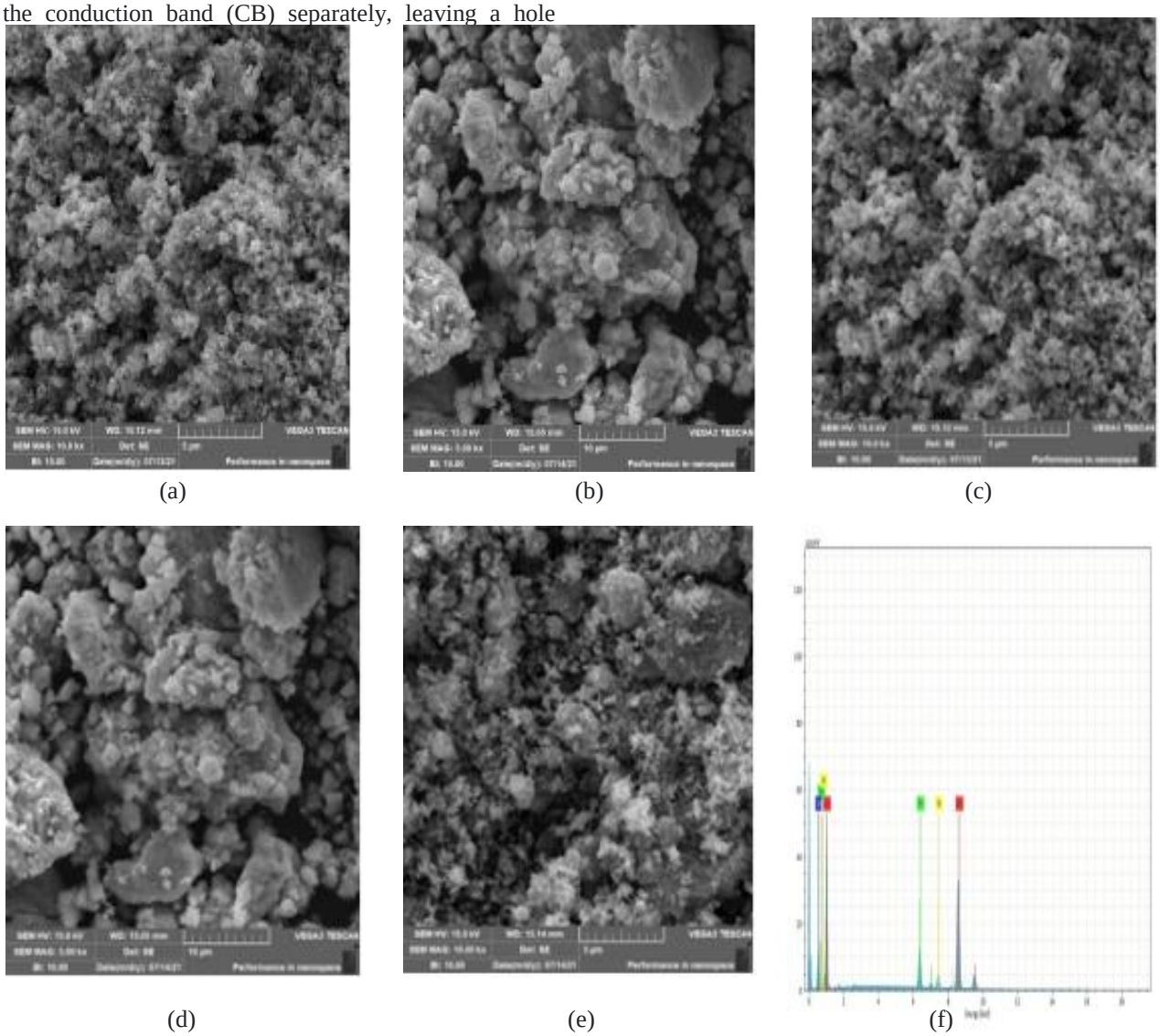

(a) (b) (c)

(d) (e) (f)

Figure 2. SEM (a) ZnO, (b) $NiFe_2O_4$, © ZNi-1, (d) ZNi-2, (e) ZNi-3, (f) EDS spectra of ZnO/$NiFe_2O_4$ nanocomposit

Photogenerated electron transfer from CB $NiFe_2O_4$ to CB ZnO and hole transfer from VB ZnO to VB $NiFe_2O_4$ will be facilitated. . The resulting electrons then react with the O_2 in the solution to form O_2 ions, which then react with H_2O to form hydroxyl radicals OH. Hydroxyl radicals are extremely active groups that degrade compounds in MB to simple compounds such as CO_2 and H_2O

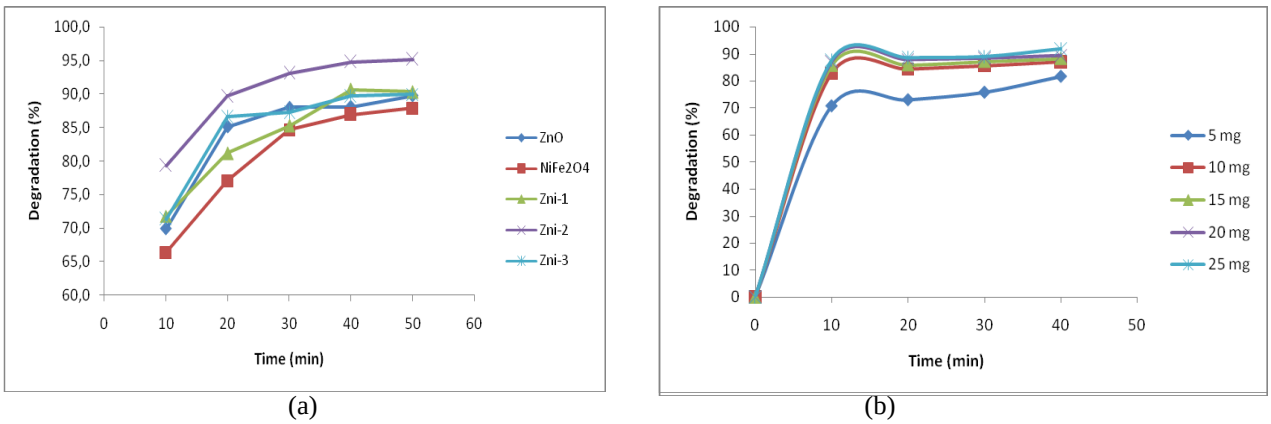

(a) (b)

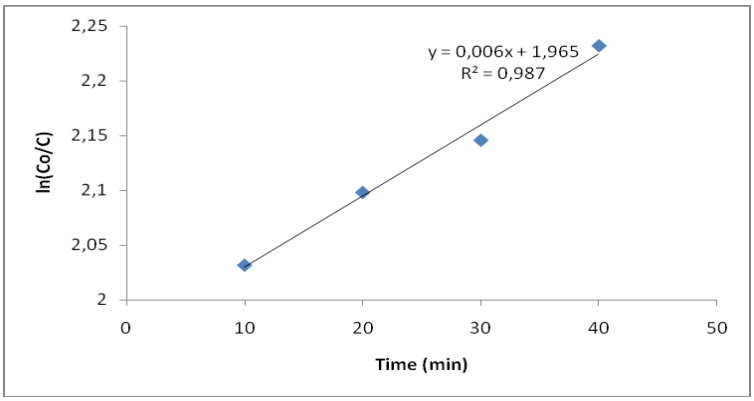

(c)

Figure 3. (a) The percentage of MB degradation under visible light (b) The percentage of MB degradation versus time in the presence of ZNi-2 the effect of catalyst loading, (b) Plot ln Co/C vs irradiation time for MB degradation using Zni-2

Catalyst loading is an important economic parameter in heterogeneous photocatalytic reactions. An experiment was carried out to determine the effect of catalyst loading on MB photodegradation by increasing the Zni-2 catalyst loading from 5 mg to 25 mg (Figure 3b). With increasing catalyst weight, the percentage of MB degradation increased. The percentage of MB degradation with a catalyst loading of 25 mg yielded the highest value of 92 percent after 40 minutes of irradiation.

This is the maximum catalyst load for MB degradation in a solution of 30 mL (50 mg/L). These materials could, of course, be used as photocatalysts to degrade methylene blue dyes in wastewater.

When adsorption occurs via interfacial diffusion, the kinetics follow the rate equation of first-order kinetics. The kinetics of the MB photocatalytic degradation reaction were also investigated, with the results shown in Figure 3c. Using a first-order kinetic rate equation model, we investigated the effect of initial MB concentration on photocatalytic degradation rate. The first-order kinetic model, according to Langmuir, is ln(Co /C) = kt, where Co is the initial concentration of MB, C is the concentration of MB at time t, and the slope of k is the rate constant [15]. The rate constant of ZNi-1 (k) shown in Figure 4 is 0.1085858 min^{-1}, and the correlation constant is R^2 = 0.987.

4. CONCLUSION

Magnetic nanocomposite for photocatalysts synthesized from ZnO/$NiFe_2O_4$ by co-precipitation method with chloride salt as starting material and water as solvent. The formation of ZnO/$NiFe_2O_4$ nanocomposites and specific ratios of Zn, Ni, Fe, and O was confirmed by structure and element analysis. The nanocomposite's microstructure revealed that it was dominated by synthesized rod-like granular. All nanocomposites had higher photocatalytic activity than ZnO and $NiFe_2O_4$, and the most excellent photocatalytic activity visible irradiation was carried out by nanocomposites with a molar ratio of ZnO: $NiFe_2O_4$ of 2:0.1. After 40 minutes of irradiation, the percentage of MB degradation with a catalyst loading of 25 mg yielded the highest value of 92 percent. As a result, if used for dye degradation under visible light, this nanocomposite has a lot of potential.

ACKNOWLEDGMENTS

The authors would like to express their gratitude to LPPM Sriwijaya University for funding this research through Hibah Unggulan Profesi 2021. The authors would also like to thank the Chemical Engineering Department's Waste Management Technology Laboratory for providing laboratory assistance.

REFERENCES

[1] B. Li, T. Liu, Y. Wang, and Z. Wang, "ZnO/graphene-oxide nanocomposite with remarkably enhanced visible-light-driven photocatalytic performance," *J. Colloid Interface Sci.*, vol. 377, no. 1, pp. 114–121, 2012, doi: 10.1016/j.jcis.2012.03.060.

[2] N. Verma, S. Yadav, B. Marí, A. Mittal, and J. Jindal, "Synthesis and Charcterization of Coupled ZnO/SnO_2 Photocatalysts and Their Activity towards Degradation of Cibacron Red Dye," *Trans. Indian Ceram. Soc.*, vol. 77, no. 1, pp. 1–7, 2018, doi: 10.1080/0371750X.2017.1417059.

[3] N. Kumar, N. S. Chauhan, A. Mittal, and S. Sharma, "TiO_2 and its composites as promising biomaterials: a review," *BioMetals*, vol. 31, no. 2, pp. 147–159, 2018, doi: 10.1007/s10534-018-0078-6.

[4] Q. Wanga, J. Liana, Q Maa, S. Zhanga, J. Hea, J. Zhongc, J. Li c, H. Huang, and B. Sua, "Preparation of carbon spheres supported CdS photocatalyst for enhancement its photocatalytic H2 evolution," *Catal. Today*, vol. 281, pp. 662–

668, 2017, doi: 10.1016/j.cattod.2016.05.013.

[5] S. S. Zhou and S. Q. Liu, "Photocatalytic reduction of CO_2 based on a CeO_2 photocatalyst loaded with imidazole fabricated N-doped graphene and Cu(II) as cocatalysts," *Photochem. Photobiol. Sci.*, vol. 16, no. 10, pp. 1563–1569, 2017, doi: 10.1039/c7pp00211d.

[6] M. Shekofteh-Gohari, A. Habibi-Yangjeh, M. Abitorabi, and A. Rouhi, "Magnetically separable nanocomposites based on ZnO and their applications in photocatalytic processes: A review," *Crit. Rev. Environ. Sci. Technol.*, vol. 48, no. 10–12, pp. 806–857, 2018, doi: 10.1080/10643389.2018.1487227.

[7] C. B. Ong, L. Y. Ng, and A. W. Mohammad, "A review of ZnO nanoparticles as solar photocatalysts: Synthesis, mechanisms and applications," *Renew. Sustain. Energy Rev.*, vol. 81, no. March 2017, pp. 536–551, 2018, doi: 10.1016/j.rser.2017.08.020.

[8] N. Zhang, S. Xie, B. Weng, and Y. J. Xu, "Vertically aligned ZnO-Au@CdS core-shell nanorod arrays as an all-solid-state vectorial Z-scheme system for photocatalytic application," *J. Mater. Chem. A*, vol. 4, no. 48, pp. 18804–18814, 2016, doi: 10.1039/C6TA07845A.

[9] S. Abbasi, F. Ahmadpoor, M. Imani, and M. S. Ekrami-Kakhki, "Synthesis of magnetic Fe_3O_4@ZnO@graphene oxide nanocomposite for photodegradation of organic dye pollutant," *Int. J. Environ. Anal. Chem.*, vol. 100, no. 2, pp. 225–240, 2020, doi: 10.1080/03067319.2019.1636038.

[10] N. Chandel, K. Sharma, A. Sudahiaka, P. Raizada, A. Hosseini-Bandegharaeic, V. Thakure, and P. Singha, "Magnetically separable ZnO/$ZnFe_2O_4$ and ZnO/$CoFe_2O_4$ photocatalysts supported onto nitrogen doped graphene for photocatalytic degradation of toxic dyes," *Arab. J. Chem.*, vol. 13, no. 2, pp. 4324–4340, 2020, doi: 10.1016/j.arabjc.2019.08.005.

[11] Rahmayeni, S. Arief, N. Jamarun, Emriadi, and Y. Stiadi, "Magnetically separable ZnO-$MnFe_2O_4$ nanocomposites synthesized in organic-free media for dye degradation under natural sunlight," *Orient. J. Chem.*, vol. 33, no. 6, pp. 2758–2765, 2017, doi: 10.13005/ojc/330608.

[12] N. Jamarun and S. Arief, "Synthesis of ZnO-$NiFe_2O_4$ Magnetic Nanocomposites by Simple Solvothermal Method for Photocatalytic Dye Degradation under Solar Light," *Orient. J. Chem.*, vol. 32, no. 3, pp. 1411–1419, 2016, doi: 10.13005/ojc/320315.

[13] J. T. Adeleke, T. Theivasanthi, M. Thiruppathi, M. Swaminathan, T. Akomolafe, and A. B. Alabi, "Applied Surface Science Photocatalytic degradation of methylene blue by ZnO/$NiFe_2O_4$ nanoparticles," *Appl. Surf. Sci.*, vol. 455, no. May, pp. 195–200, 2018, doi: 10.1016/j.apsusc.2018.05.184.

[14] D. K. Huy, T. T. L. , Nguyen Phuc Duong,*, and V. V. K. Chung, Hoang Manh, Nguyen Kim Thanh, "Synthesis and Characterization of FeO_4/ ZnO core-shell Nanocomposites," *VNU J. Sci. Math. – Physics*, vol. 34, no. 4, pp. 35–43, 2018.

[15] H. Y. Zhu, R. Jiang, Y. Q. Fu, R. R. Li, J. Yao, and S. T. Jiang, "Novel multifunctional $NiFe_2O_4$ /ZnO hybrids for dye removal by adsorption, photocatalysis and magnetic separation," *Appl. Surf. Sci.*, vol. 369, pp. 1–10, 2016, doi: 10.1016/j.apsusc.2016.02.025.